PCCP

ROYAL SOCIETY OF CHEMISTRY

PAPER

View Article Online
View Journal | View Issue

Cite this: *Phys. Chem. Chem. Phys.*, 2022, **24**, 15083

High temperature molecular motions within a model protomembrane architecture†

Loreto Misuraca,[ab] Tatsuhito Matsuo,[abc] Aline Cisse,[ab] Josephine LoRicco,[d] Antonio Caliò,[d] Jean-Marc Zanotti,[f] Bruno Demé,[b] Philippe Oger *[d] and Judith Peters *[abe]

Received 12th March 2022,
Accepted 8th June 2022

DOI: 10.1039/d2cp01205g

rsc.li/pccp

Modern phospholipid membranes are known to be in a functional, physiological state, corresponding to the liquid crystalline phase, only under very precise external conditions. The phase is characterised by specific lipid motions, which seem mandatory to permit sufficient flexibility and stability for the membrane. It can be assumed that similar principles hold for proto-membranes at the origin of life although they were likely composed of simpler, single chain fatty acids and alcohols. In the present study we investigated molecular motions of four types of model membranes to shed light on the variations of dynamics and structure from low to high temperature as protocells might have existed close to hot vents. We find a clear hierarchy among the flexibilities of the samples, where some structural parameters seem to depend on the lipid type used while others do not.

Introduction

The onset of first cellular life on Earth goes back to about 4 billion years.[1] Therefore, the origin and nature of the first cell membranes and their constituents are not fully determined. Because of the supposed lack of molecular complexity on the early planet, the first cell membranes were most likely composed of simple, single chain fatty acids[2] and fatty alcohols, raising questions as how they could withstand the very variable and extreme surrounding environment[3] of the oceanic hydrothermal vents or fields. One of the commonly accepted scenarios for the origin of life is indeed related to such places.[4] In particular, the membranes may have had to cope with high temperatures (typically around 85 °C) and high hydrostatic pressures (up to a few hundred bars), and simultaneously accomplish elementary but crucial functions of cell membranes: divide the inside and outside into separate compartments, and assure a limited permeability combined with a certain stability and flexibility.

As proto-cells or proto-membranes are no longer accessible due to evolution, the only way to probe the properties of these hypothetical systems is to re-construct membranes from simple lipids with short chain lengths, presumably favoured by prebiotic synthesis,[5–7] and to expose them to the supposed environmental conditions. Here we concentrate on fatty acids, fatty alcohols and phospholipids, all with chain lengths of 10 carbons (named hereafter C10), which are among the shortest to self-assemble into lipid bilayers.[8,9]

Specifically, we study here several possibilities (see Fig. 1): first, decanoic (or capric) acid, which is a C10 fatty acid known to form vesicles under fixed conditions.[9] Second, a possible architecture for protocell membranes, consisting of a 1:1 mixture of capric acid with a fatty alcohol of equal chain length (decanol). These short, single chain amphiphilic molecules were in fact the ones readily available in the prebiotic environment and have been found able to form stable vesicles.[10] In a recent work, we reported the remarkable properties of this membrane architecture which allow it to withstand extreme temperature conditions.[11] Indeed, such a combination of fatty acids and alcohols improves the vesicles' stability at room

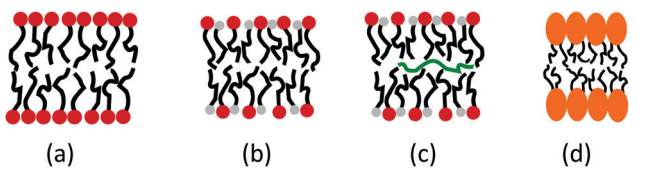

Fig. 1 Four models for protomembranes: (a) capric acid, (b) capric acid + decanol (C10mix), (c) C10mix + eicosane, (d) DCPC.

[a] *Univ. Grenoble Alpes, CNRS, LIPhy, 38000 Grenoble, France. E-mail: jpeters@ill.fr*
[b] *Institut Laue Langevin, F-38042 Grenoble Cedex 9, France*
[c] *Institute for Quantum Life Science, National Institutes for Quantum Science and Technology, 2-4 Shirakata, Tokai, Ibaraki, 319-1106, Japan*
[d] *INSA Lyon, Université de Lyon, CNRS, UMR5240, Villeurbanne, France. E-mail: philippe.oger@insa-lyon.fr*
[e] *Institut Universitaire de France, France*
[f] *Laboratoire Léon Brillouin, CEA, CNRS, Université Paris-Saclay, CEA Saclay, 91191 Gif-sur-Yvette Cedex, France*

† Electronic supplementary information (ESI) available: Includes figures of the amplitudes A_0 to A_3 of all samples at 278, 293, 323 and 353 K, of the fits of the HWHM Γ_1 to Γ_3 of all samples as function of Q^2 and temperature and of the fits of the amplitudes for all four samples. See DOI: https://doi.org/10.1039/d2cp01205g

temperature and it induces a high-temperature conformational change at $T \geq 60$ °C that leads to vesicle fusion with stable membranes at temperatures as high as 80 °C. In the following, this model membrane will be referred to as C10mix.

The third model is inspired by the work of Cario *et al.*[12] These authors proposed an important role of long chain isoprenoid alkanes (referred as "apolar lipid") in the membrane midplane to further trigger its physico-chemical properties in relation to extreme conditions. In fact, Salvador-Castell *et al.* did find that they had a stabilizing role in model archaeal membranes[13] and Misuraca *et al.* reported an increased stability of lipid membranes in presence of alkanes.[14,15] Thus the C10mix was enriched with small percentages of eicosane, a linear alkane with 20 carbons (C20). The C10mix containing eicosane can be considered as the most complete prebiotic model that sums up the requested features of molecular abundance and need for a strategy against high temperature.

To further compare the decanoic acid to a more evolved lipid, a phospholipid having two C10 acyl chains, but a much larger choline headgroup, was chosen: 1,2-didecanoyl-*sn-glycero*-3-phosphocholine (DCPC). The acyl chains are bound to the headgroup through a glycerol backbone, which can stiffen the structure.

Not only the structural composition of lipidic membranes is significant for their behavior, but their dynamic properties have an equally important impact.[16] High temperature is known to increase the thermal energy and thus molecular motions within membranes, hence jeopardizing the stability of the system. Nonetheless, to be functional a cell membrane requires a specific state of fluidity and therefore high flexibility. Both together can be ensured by molecular dynamics within the membranes.

Many kind of motions were identified within lipidic membranes, from small local motions up to collective motions of the whole system. A well adapted technique for their observation and analysis is incoherent neutron scattering, which probes essentially the motions of hydrogen atoms and of the molecular subgroups to which they are bound.[17–20] Neutron instruments give access to a broad range of energy resolutions, which are inversely propotional to the accessible time window, and thus allow different types of motions to be probed. In the present study, we combine elastic incoherent neutron scattering (EINS) experiments giving access to atomic mean square displacements (MSD) with quasi-elastic neutron scattering (QENS) experiments to characterize the kind of motion present in the sample and the associated amplitudes. To the best of our knowledge, such complete investigation on multilamellar vesicles of one type of lipids, of mixed lipids and alcohol or in presence of alkanes was never attempted before, mainly due to the lack of a suitable model to describe the dynamics. However, as molecular dynamics are so important for the understanding of the correct functioning in a certain state, we show here which parameters can be extracted, which ones are the most impacted by the structural differences and how we can interpret these variations.

Experimental section

Sample preparation

Decanoic acid, 1-decanol, perdeuterated eicosane, DCPC, bicine buffer and D_2O were purchased from Sigma Aldrich (Merck). The samples were prepared by dissolving the decanoic acid and the decanol in a $CHCl_3$ solution and DCPC in chloroform:-methanol (2 : 1), followed by drying under a stream of nitrogen. The samples were then placed in a desiccator and left under vacuum overnight. The sample weights were checked at each step, to make sure that all the organic solvent was evaporated. For the samples consisting of decanoic acid: 1-decanol (C10mix) the final ratio was 1 : 1.

The bicine buffer was prepared at a concentration of 0.2 M by dissolving hydrogenated bicine in D_2O, following previous protocols.[10] The buffer was filtered with a 0.2 μm millipore membrane before use. The dried organic solutions were then resuspended in buffer by vigorous vortexing for ≈1 min, leading to the final milky-foamy solutions characteristic of the presence of large multi-lamellar vesicles (MLVs). The samples to be measured were then diluted in D_2O buffer to a final concentration of 60 mg ml^{-1} (350 mM). The samples were placed in flat aluminium sample holders and sealed with indium. Their weights were checked before and after the experiment to control that no solution was lost.

Incoherent neutron scattering

The incoherent neutron scattering cross section of hydrogen exceeds by far that of all other atoms present in biological systems[21] and also that of its isotope deuterium. Therefore, contrast variation can be used to highlight specific parts of the samples, as in our case the lipids rather than the buffer or the alkanes, whose presence will only be accounted for by their impact on the membrane dynamics.

For our study, we used the spectrometer IN6-Sharp operated by the Laboratoire Léon Brillouin (Saclay, France) at the Institut Laue Langevin (ILL) in Grenoble, France. IN6-Sharp is a cold neutron time-of-flight[22] with an energy resolution of 70 μeV at 5.1 Å incident wavelength, giving access to a time window of about 10 ps. Elastic scans were performed from 278 to 355 K with a temperature step of 1 K and a measuring time of 2 minutes per point. QENS measurements were conducted on the same samples at the temperature points of 278, 293, 323 and 353 K for 2.5 hours each. Additionally, the bicine buffer was measured in the same conditions with the exception that the QENS scans were acquired for only 2 hours due to time limitations. An empty cell and the completely incoherent scatterer vanadium were measured at room temperature for correction and normalisation purposes. The empty cell and buffer data were subtracted from the sample data taking into account their different absorptions based on the correction formula of Paalman–Pings coefficients.[23] Vanadium data were used to normalise the elastic data and to determine the instrumental resolution for QENS data. Data reduction for EINS was carried out using the LAMP software[24] available at ILL and using the IGOR Pro software (WaveMetrics, Lake Oswego, OR, USA) for QENS.

Elastic incoherent neutron scattering

EINS measurements give access to the elastic incoherent structure function $S(Q, 0 \pm \Delta E)$, where Q is the modulus of the difference between the incoming and outgoing neutron wavevectors and ΔE the energy resolution of the instrument. The structure factor can be written, using the Gaussian approximation,[25] which assumes that the distribution of the atoms around their average position follows a Gaussian distribution,

$$S(Q, 0 \pm \Delta E) \approx e^{-\frac{1}{3}\langle u^2\rangle Q^2}, \quad (1)$$

where the $\langle u^2\rangle$ are the MSD. As Q approaches zero, the approximation is strictly valid and it holds up to $\langle u^2\rangle Q^2 \approx 1$.[26]

The average MSD can be obtained from the slope of the logarithm of the scattered intensities according to

$$\langle u^2\rangle = -3\frac{\partial(\ln S(Q, 0 \pm \Delta E))}{\partial Q^2}. \quad (2)$$

The Q-range used for fitting was on IN6-Sharp 0.45 to 1.4 Å^{-1}. It is possible to further determine the force constant or resilience $\langle k\rangle$ from the slope of the MSD[27] through

$$\langle k\rangle = \frac{k_B}{\frac{d\langle u^2\rangle}{dT}}, \quad (3)$$

where k_B is Boltzmann's constant.

Quasi-elastic neutron scattering

Whereas elastic scattering permits only averaged local motions to be seen, QENS is the tool to separate different kind of movements and to characterize them. For that, each spectrum can be fitted after the data reduction with a phenomenological equation containing terms which account for various diffusions:

$$S(Q,\omega) = C(Q)\left[A_0(Q)\delta(\omega) + \sum_i A_i(Q)L_i(Q,\omega)\right] \times R(Q,\omega) + B(Q), \quad (4)$$

where ω is the energy transfer in multiples of $\hbar$, *C(Q)* is a scaling factor to adjust the model and the absolute data, and $A_0(Q)\ \delta(\omega)$ is the Q-dependent elastic incoherent structure factor (EISF). The functions $L_i(Q,\omega)$ are Lorentzian functions of half-width at half-maximum (HWHM) Γ_i, each describing a certain type of diffusive motion in the lipids. Their amplitudes $A_i(Q)$ are also Q-dependent. $R(Q,\omega)$ refers to the instrumental resolution which is obtained from the vanadium measurements. $B(Q)$ is a flat background. The sum can theoretically be extended over an infinity of contributions, but real data allow only to resolve a few of them. Careful checks determined that 3 Lorentzians were sufficient to reasonably fit the data here without overfitting them. They represent slow (*e.g.* two-dimensional diffusion within the membrane plane and one-dimensional diffusion of the whole lipid perpendicular to the plane), intermediate (*e.g.* jump diffusion, flip–flop and rotational motions of the headgroup) and fast motions (*e.g.* small vibrations), as classified in the Matryoshka model recently proposed for a very complete description of motions within a membrane.[28]

The behaviour of Γ as function of Q^2 is indicative for the type of movement:[29] a linear behaviour represents translational diffusion characterized by the diffusion coefficient D_T:

$$\Gamma = D_T Q^2. \quad (5)$$

Sometimes, Γ is not crossing the origin for $Q \to 0$, signature of confinement for larger amplitudes. In this case, it is advised to fit the data only from a Q_{min} on, where the linear behaviour sets in.

A constant behaviour found for Γ, in particular at higher energies meaning at very short times, is characteristic for fast vibrational motions. Knowing the structure of lipid molecules, they could be interpreted in terms of vibrations of CH_2-groups in the tails.

Finally, jump-diffusion,[30] characterised by the jump diffusion coefficient D_{jump}, is typical for infinitely small, elementary jumps and a certain time spent by the protons in between, the residence time τ. Here, Γ as function of Q^2 increases towards a constant limit, $\Gamma_\infty = 1/\tau$:

$$\Gamma = \frac{D_{jump}Q^2}{1 + D_{jump}Q^2\tau}. \quad (6)$$

It is moreover possible to calculate an equivalent jump length[31] through

$$l = \sqrt{2D_{jump}\tau} \quad (7)$$

accounting for confined jump diffusion within the lipid tail inside the membrane.

We fitted the experimental spectra in the Q-range from 0.37 to 2.02 Å^{-1} and within energy transfers ω from −10 meV to 2 meV (see an example in Fig. 2).

Results and discussion

Experiments were performed in August 2020 on IN6-Sharp (DOI: 10.5291/ILL-DATA.CRG-2728).

EINS

The integration of the elastic peak allowed the extraction of the MSD as a function of temperature through eqn (2) (see Fig. 3). Generally speaking, lipids are very flexible molecules and our results are in close agreement with other examples in the literature (see ref. 32, but note that in this reference the use of a different factor for the MSD).

The slopes ($\langle k\rangle$) of all four curves present very similar trends (see Table 1), indicating that the four systems have similar stabilities. On the contrary, the MSD data highlights a few particularities for each one. As can be seen in Fig. 3, the C10mix is the most flexible sample over the whole temperature range. However, we do not observe an impact of the conformational transition of the C10mix above 333 K on the local dynamics as seen by DLS,[11] likely due to the different time scales of the two techniques. By contrast, the capric acid seems to undergo a

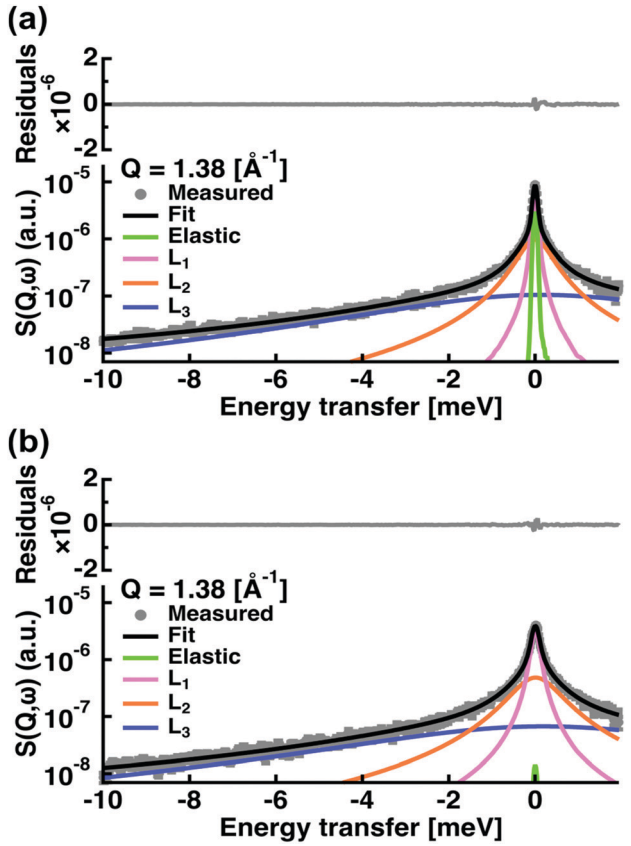

Fig. 2 Examples of fit results for the spectra of (a) capric acid and (b) C10mix, both at Q = 1.38 Å^{-1} and T = 293 K. The grey circles are the data points with errors, the black line is the total fit line. The green line represents the elastic contribution convoluted by the resolution function. The magenta, orange and blue curves are the Lorentzian functions corresponding to slow, intermediate and fast motions, respectively, convoluted by the resolution.

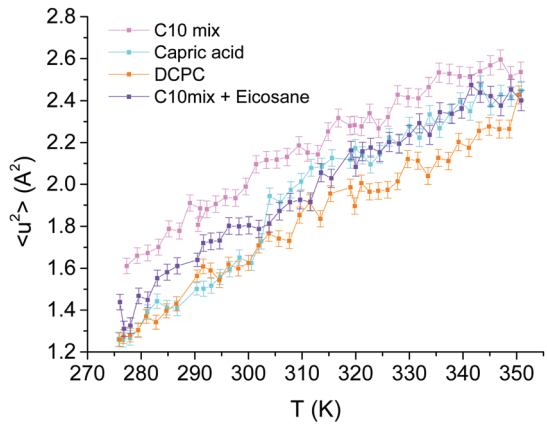

Fig. 3 MSD for MLVs of the four samples as a function of temperature.

steep raise in MSD at around 305 K, indicative of a phase transition, which is somewhat higher than the one observed by DSC in previous studies (287 K).[11,14] We interpreted the phase at lower temperature as a collapsed phase, which melts around this temperature.[11] The shift in temperature observed here can have various reasons such as different temperature ramps for the two techniques or differences in hydration.[32]

Table 1 The force constants of the four samples

	$\langle k \rangle$ (N m^{-1})
C10mix	0.102 ± 0.003
C10mix + eicosane	0.092 ± 0.002
DCPC	0.096 ± 0.002
Capric acid (<305 K)	0.085 ± 0.005
Capric acid (>305 K)	0.124 ± 0.007

In presence of eicosane, the C10mix becomes less flexible, as expected due to the hindrance of motions by an obstacle in the midplane of the bilayer, but as mentioned above, it maintains a stability similar to the C10mix as indicated by the slope values. Finally, DCPC presents the lowest MSD, only coinciding with those of capric acid at the lowest temperatures. The bigger headgroups, and the connection of the two C10 chains to the glycerol backbone could indeed hinder motions at the level of the heads or within the hydrophobic region.

QENS

The treatment of the QENS data gave access to different information: first, we extracted the amplitudes A_0 to A_3 of all samples (see Fig. S1–S4 in the ESI†). The amplitude A_0 or EISF represents, at the highest Q value available, the proportion of particles seen as immobile within the instrumental resolution. At the two highest temperatures, 323 and 353 K, all four curves converge quickly to zero at higher Q values, indicating the high mobility. At the lower temperatures, capric acid and DCPC present values between 0.05 and 0.02 showing that not all hydrogens are participating in the motions yet. Capric acid has the highest values for these temperatures, but joins the other curves in between 293 and 323 K, in accordance with the phase transition found from EINS. The C10mix seems again the most flexible, but very similar to its counterpart with eicosane. The amplitudes A_0 to A_3 will be treated in more detail with the Matryoshka model[28] to extract also structural information (see below).

Second, the HWHM Γ_i are representative of three identified types of motions (see Fig. S5–S7 in the ESI†). It can be deduced by the different energy ranges they cover: approximately from 0.05 to 0.35 meV for Γ_1 (corresponding to a time window of 2–13 ps), from 0.25 to 1.25 meV for Γ_2 (0.5–2.6 ps) and from 3 to 8 meV for Γ_3 (0.08–0.2 ps). From their behaviours as a function of Q^2, one identifies that Γ_1 corresponds to continuous diffusional motions, including confinement for C10mix and C10mix + eicosane, Γ_2 to jump diffusion and Γ_3 to small vibrations. The values of Γ_2 also fluctuate sensibly below the Q-value of 1.1 Å^{-1} around an almost constant value. Such attitude is indicative of a confined motion, which can be characterized by a radius of confinement a, to be determined through $a = \pi/Q_0$, where Q_0 stands for the momentum transfer where jump diffusion sets in. In the present cases, this critical value of Q_0 = 1.1 Å^{-1} was the same for all samples and thus a equals to 2.9 Å.

With respect to the global translational diffusion coefficient ($D_1 = D_T$), which corresponds to motions of lipids within the

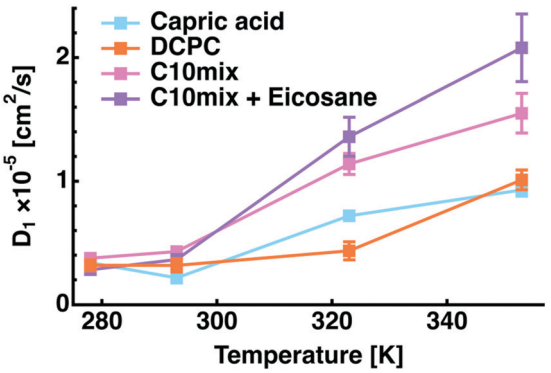

Fig. 4 Global translational diffusion coefficient of all four samples as a function of temperature.

membranes (see eqn (5)), as shown in Fig. 4 as a function of temperature, it seems to be very similar for all four samples at 278 and 293 K. At 323 and 353 K, the diffusion coefficients of Capric acid and DCPC stay very similar, but those of C10mix and C10mix + eicosane raise considerably. This effect is also present in the curves of Γ_1 as function of Q^2, where the line widths are almost constant below Q_0 = 1.1 Å^{-1} for these two samples, likely because the large amplitudes of motions of the acyl chains are limited by confinement by the environment. Above Q_0, pure translational diffusion is present. All values of the diffusion coefficients are in between 0.3 × 10^{-5} cm^2 s^{-1} at 278 K and 2 × 10^{-5} cm^2 s^{-1} at 353 K and lie below the value of bulk water, 2.3 × 10^{-5} cm^2 s^{-1} at 298 K and 6.81 × 10^{-5} cm^2 s^{-1} at 353 K,[33] which represents somehow the upper limit for such diffusional processes. They are on the contrary of the same order of magnitude as the diffusion coefficients found for the phospholipids 1,2-dimyristoyl-*sn-glycero*-3-phosphocholine (DMPC) and 1,2-dimyristoyl-*sn-glycero*-3-phospho-(1′-*rac*-glycerol) (DMPG)[34] in the same temperature range. The reason why D_1 is smaller for Capric acid and DCPC might be the absence of decanol, as the fatty alcohol might fluidize more the membrane, as partly corroborated by the increased MSD values for C10mix compared with Capric acid (Fig. 3), and the bigger headgroup for DCPC, which could hinder certain motions. The vesicles of Capric acid and C10mix are known to show different structural behaviour in solution as a function of temperature.[11] For example, C10mix starts to undergo vesicular fusion above 323 K while Capric acid does not show such a transition. Furthermore, even at the same ambient temperature, the size and distribution of the vesicles are largely different between Capric acid and C10mix. Although the current sample conditions are not exactly the same as those of the previous study, the above structural differences would cause confinement effects on C10mix with or without eicosane as observed at higher temperatures (Fig. 4).

The second type of motion corresponds to jump diffusion and allows the determination of the jump diffusion coefficient ($D_2 = D_{\text{jump}}$) and residence time according to eqn (6). Fig. 5 represents these quantities for all samples. However, this model does not describe very well the motions within C10mix + eicosane and DCPC, leading to huge error bars. We can speculate that 2, 3-site jump diffusion could be more appropriate

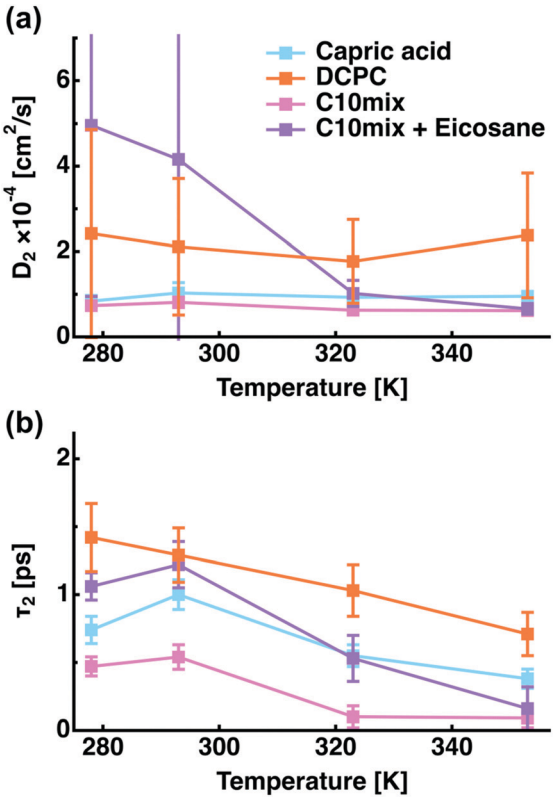

Fig. 5 The jump diffusion coefficient and the residence time for all samples as a function of temperature extracted from Γ_2.

here. The equivalent jump length l (eqn (7)) results in distances of about 1–2 Å, supposing a diffusion coefficient of about 2 × 10^{-4} cm^2 s^{-1} and a residence time of 0.5–1 ps. These values can be attributed to H-atoms of the methylene groups CH_2, with jump distances of ≈1.8 Å between the H positions and such typical residence times.[16]

The hierarchy of the residence times is consistent with the EINS results, *e.g.* C10mix < capric acid < C10mix + eicosane < DCPC. This quantity, representative for interactions between molecules, decreases with temperature as the lipids become more and more mobile and is highest for DCPC.

The last contribution Γ_3 is almost flat and thus compatible with harmonic vibrations, probably again arising from CH_2 groups in the lipid tails. These very small and fast motions can be resolved due to the high dynamic range of IN6 – Sharp and are almost not prone to the specific environment and temperature.

We further used a recently developed model to interpret the amplitudes A_0 to A_3 of eqn (4), the Matryoshka model[28] (see Fig. 6). Although the Matryoshka model is dynamic, fitting the data with it, starting from values found in the literature, it allows to determine the impact of molecular dynamics on certain structural parameters. The amplitudes are globally fitted for each sample, but independently for each temperature point.

The Matryoshka model describes the two alkyl chains as one and the same cylinder. The modelled parameters are the following: R is the lateral diffusion radius of the whole lipid in the membrane plane. k_{force} represents a force constant or resilience characterising the relaxation of the lipid with respect

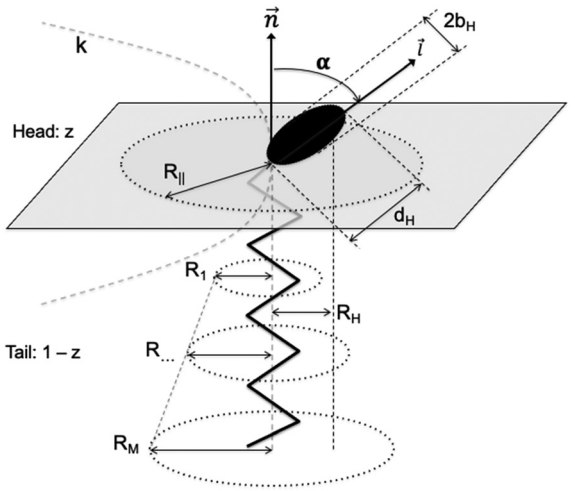

Fig. 6 Representation of a lipid molecule within the Matryoshka model and fit parameters.

to out-of-plane motions. The whole lipid can rotate, expressed through the distance head-lipid R_H. Flip–flop motions of the head group are described by the angle α (we are using the definition of Pfeiffer *et al.*[17] and not the exchanges of lipids from one layer to the other, which correspond to much longer time scales) and the heads with radius b_H can rotate around their own axis. R_1 stands for the minimum radius of diffusion of the lipid tail, which according to the distance from the head increases with $\sqrt{m}$, m being the index of the methylene group position on the tail and M the total number of these groups (here: M = 10 for all samples). H atoms inside the methylene and methyl groups can undergo jump-diffusion. The parameters needed to describe these motions are the distance H–C–H d between the two-sites and the probability of jump events ϕ. The model depends further on experimental parameters known for lipids as the number z, which is the proportion of H atoms in the head (here z = 0.05 for capric acid, =0.03 for C10mix with and without the eicosane, =0.32 for DCPC) and on the fraction of H atoms, seen as immobile within the instrumental resolution, termed here p_{imm}. For a validation of the model upon real data, see.[34,35]

In Fig. S8 of the ESI† we show the fits of the amplitudes for all four temperatures of our samples. Globally, they work remarkably well, giving mainly rise to reduced χ^2 values between 1 and 16. This is as more satisfying as the model was first developed for phospholipids and successfully applied here for a first time to single chain fatty acids and alcohols, too.

The extracted fit parameters are presented in Fig. 7. Some remarks are noteworthy: when z has a very small value (as here for capric acid and C10mix), it is almost impossible to model the head motions, which explains the huge error bars for parameters b and α for these samples. For DCPC, α was fixed to 30°, similarly to the tilt angle of DMPC, as the head groups are the same.[35] In that case, the error bars are smaller and b is in the same order of magnitude as for DMPC,[35] which is consistent with identical head groups. The other quantity for which the fits cannot give reliable results is the tilt angle α. In fact, the head group of capric acid and C10mix is so small that its orientation does not make sense.

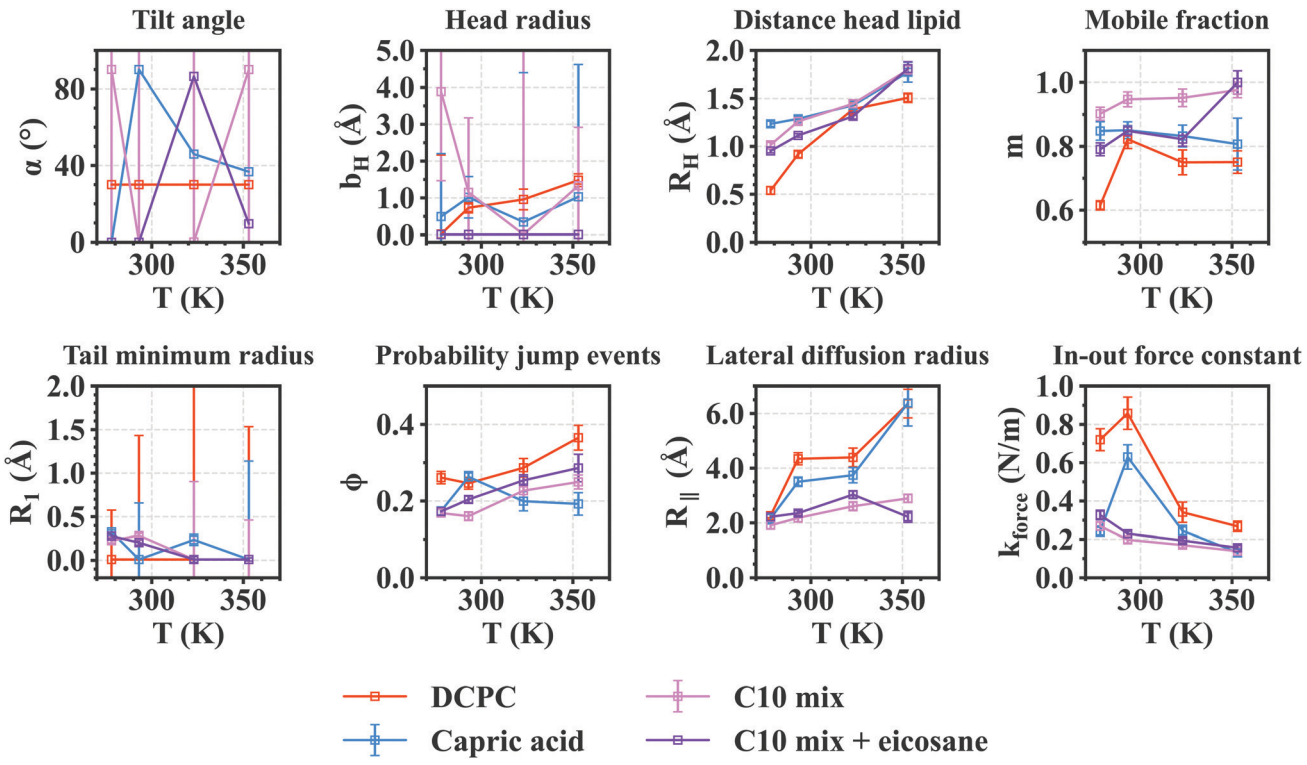

Fig. 7 Fit parameters obtained for all samples as a function of temperature. Error bars are within symbols if not shown.

In contrast to DMPC,[27] R_1 is close to 0 for almost every sample, meaning that the corresponding motion, the 2D diffusion of the effective tail, is negligible compared to the jump-diffusion of methyl groups. As it occurs for all systems with different head groups, this is probably related to the smaller chain length (M = 10, compared to M = 14 for DMPC), which would hinder the 2D diffusion of the tail. However, R_1 seems slightly bigger for DCPC, which can be assigned to the lower phase transition temperature of DCPC so that these lipids are in a liquid crystalline state even at 293 K.

The jump-diffusion, represented by the ϕ parameter, seems to be more likely to occur in DCPC, and much less in capric acid. This could be due to the larger head group and the liquid crystalline state of DCPC, allowing more motions within the chains, or to the fact that there are two tails in DCPC, compared to one in all other systems, and one effective tail considered in the Matryoshka model (as discussed by Bicout *et al.*[16]). Eicosane does not seem to have a strong effect on this parameter, which is reasonable as it is supposed to be mainly in the midplane of the bilayers, and thus is not supposed to interact with the majority of methylene and methyl groups.

Overall, the fraction of mobile H atoms is similar for all samples, and is about 80%. Notably, the hierarchy between the samples is close to the one encountered for the MSD in Fig. 3, where the C10mix displays the highest mobile fraction, and DCPC the lowest. We also retrieve the lowering effect of eicosane, with a decrease in the mobile fraction, except for the highest temperature.

Concerning the motions of the whole lipid, we can first comment on the rotation, corresponding to the parameter R_H. While increasing with temperature, following the increase in thermal energy, the values of R_H stand for all samples around 1.5 Å, which can be put in comparison with measurements by SANS and NMR. Indeed, they give an estimated value for the distance between the lipid axis $\vec{n}$ and the center of inertia of all H-atoms with respect to $\vec{n}$ (see Fig. 6) of 1.7 Å.[11] Here R_H corresponds to a projection of this quantity, which is then supposed to be lower. It is slightly smaller for DCPC than for the other samples, because the single chain amphiphiles will rotate along their longitudinal axis much more easily than DCPC.[36]

For the lateral diffusion radius and the in-out force constant, one recognises two groups, formed by DCPC and capric acid on one side and C10mix with or without eicosane on the other side. We can conclude that in the latter case, in-plane motions of the lipids are more restricted, but the membrane is more flexible in the out-of-plane direction. The presence of eicosane can certainly explain such behaviour, but it seems already present in the C10mix alone. One might speculate that it favours the requirements of a protomembrane.

Conclusions

In summary, the exact composition of the lipid model membrane has a clear effect on molecular dynamics and structural parameters. EINS established the existence of a phase transition around 305 K for capric acid, likely corresponding to the melting of a collapsed phase already seen earlier.[11] Otherwise we found the following hierarchy in the flexibilities with C10mix > capric acid > C10mix + eicosane > DCPC, although the stabilities (determined by the force constants, Table 1) were very similar for all of them. It fosters the idea that the C10mix permits a high degree of adaptation to the environment due to the flexibility, which is however slightly decreased by the presence of the alkanes located in the midplane. As shown earlier,[14,15] the alkanes on the contrary increase the membrane's stability under extreme temperature and pressure conditions.

QENS measurements revealed that the C10mix sample containing eicosane presented a very high translational diffusion at the highest temperature (which is supposed to correspond to the native conditions). In contrast to that, the jump diffusional coefficient, characteristic of smaller localised motions, of this sample evolved from a high value at low temperature to the same value as for capric acid and C10mix alone at high temperature. Thus such a small value seems mandatory for a good functioning. All these values are quite different from those of DCPC, which is a non-prebiotic phospholipid with a much bigger headgroup. The small vibrations, represented by the widths of the third Lorentzian, are not sensitive to their environment or to temperature and are the same for all samples.

The amplitudes of the motions permitted further structural parameters to be obtained through a fitting procedure with some starting values taken from the literature, as observed through the dynamical changes. The two parameters b and α are not well defined for capric acid and C10mix due to their small head groups and are fixed for DCPC. Some parameters, such as R_H, R_1 and φ do not differ significantly among the samples. On the contrary, m, $R_\parallel$ and k_{force} show respectively two groups of samples, assembling capric acid and DCPC on one side and C10mix and C10mix with eicosane on the other side. So one might speculate that these three parameters are the most important to guarantee the good functioning of a membrane built from short-chain lipids and alcohol, with or without alkanes in the midplane. We retain a higher mobile fraction for these samples, especially at higher temperature, paired with a smaller lateral diffusion radius and a lower in-out force constant, indicating the motional direction perpendicular to the surface being favoured over lateral motions. The EINS data showed in addition that the C10mix has a slightly lower flexibility albeit the same stability as C10mix, so that these characteristics seem to be optimal paired with the suitable permeability studied earlier.[13]

Conflicts of interest

There are no conflicts to declare.

Acknowledgements

This work was funded by the French National Research Agency program ANR 17-CE11-0012-01 to P. O. and J. P. L. M. was supported by a scholarship from the Institut Laue-Langevin

(ILL) PhD program. The authors thank ILL for neutron beamtime on IN6-Sharp (DOI: 10.5291/ILL-DATA.CRG-2728).

References

1 E. A. Bell, P. Boehnke, T. M. Harrison and W. L. Mao, *Proc. Natl. Acad. Sci. U. S. A.*, 2015, **112**, 14518–14521.
2 P. A. Monnard and D. W. Deamer, *Methods Enzymol.*, 2003, **372**, 133–151.
3 K. Morigaki and P. Walde, *Curr. Opin. Colloid Interface Sci.*, 2007, **75**, 80.
4 M. S. Dodd, D. Papineau, T. Grenne, J. F. Slack, M. Rittner, F. Pirajno, J. O'Neil and C. T. Little, *Nature*, 2017, **543**, 60–64.
5 B. R. Simoneit, *Adv. Space Res.*, 2004, **33**, 88–94.
6 G. U. Yuen and K. A. Kvenvolden, *Nature*, 1973, **246**, 301–303.
7 I. Budin, N. Prywes, N. Zhang and J. W. Szostak, *Biophys. J.*, 2014, **107**, 1582–1590.
8 D. Deamer, *Life*, 2017, 7.
9 C. L. Apel, D. W. Deamer and M. N. Mautner, *Biochim. Biophys. Acta, Biomembr.*, 2002, **1559**, 1–9.
10 S. Kapoor, M. Berghaus, S. Suladze, D. Prumbaum, S. Grobelny, P. Degen, S. Raunser and R. Winter, *Angew. Chem., Int. Ed.*, 2014, **53**, 8397–8401.
11 L. Misuraca, A. Calio, I. Grillo, A. Grelard, P. M. Oger, J. Peters and B. Demé, *Langmuir*, 2020, **36**, 13516–13526.
12 A. Cario, V. Grossi, P. Schaeffer and P. M. Oger, *Front. Microbiol.*, 2015, 6.
13 M. Salvador-Castell, M. Golub, N. Erwin, B. Demé, N. J. Brooks, R. Winter, J. Peters and P. M. Oger, *Commun. Biol.*, 2021, **4**, 653.
14 L. Misuraca, B. Demé, P. Oger and J. Peters, *Commun. Chem.*, 2021, **4**(24), 21–28.
15 L. Misuraca, A. Calio, J. G. LoRicco, I. Hoffman, R. Winter, B. Demé, J. Peters and P. M. Oger, *Life*, 2022, **12**, 445.
16 W. Knoll, J. Peters, P. Kursula, Y. Gerelli, J. Ollivier, B. Demé, M. Telling, E. Kemner and F. Natali, *Soft Matter*, 2014, **10**, 519–529.
17 S. König, W. Pfeiffer, T. Bayerl, D. Richter and E. Sackmann, *J. Phys.*, 1992, **2**, 1589–1615.
18 W. Pfeiffer, T. Henkel, E. Sackmann, W. Knoll and D. Richter, *Europhys. Lett.*, 1989, **8**, 201–206.
19 U. Wanderlingh, G. D'Angelo, C. Branca, V. C. Nibali, A. Trimarchi, S. Rifici, D. Finocchiaro, C. Crupi, J. Ollivier and H. D. Middendorf, *J. Chem. Phys.*, 2014, **140**, 174901.
20 S. Gupta, J. U. DeMel and G. J. Schneider, *Curr. Opin. Colloid Interface Sci.*, 2019, **42**, 121–136.
21 V. F. Sears, *Neutron News*, 1992, **3**, 26–37.
22 **https://www.ill.eu/users/instruments/instruments-list/sharp/description/instrument-layout**.
23 H. H. Paalman and C. J. Pings, *J. Appl. Phys.*, 1962, **33**, 2635–2639.
24 D. Richard, M. Ferrand and G. J. Kearley, *J. Neutron Res.*, 1996, **4**, 33–39.
25 A. Rahman, K. S. Singwi and A. Sjolander, *Phys. Rev.*, 1962, **126**, 986–996.
26 V. Réat, G. Zaccai, C. Ferrand and C. Pfister, inproceedings, 1997.
27 G. Zaccai, *Science*, 2000, **288**, 1604–1607.
28 D. J. Bicout, A. Cisse, T. Matsuo and J. Peters, *Biochim. Biophys. Acta, Biomembr.*, 2022, 183944.
29 M. Bée, *Quasielastic Neutron Scattering:Principles and Applications in Solid State Chemistry, Biology and Materials Science*, Adam Hilger, Philadelphia, 1988.
30 K. S. Singwi and A. Sjölander, *Phys. Rev.*, 1960, **119**, 863–871.
31 P. L. Hall and D. K. Ross, *Mol. Phys.*, 1981, **42**, 673–682.
32 B. Aoun, E. Pellegrini, M. Trapp, F. Natali, L. Cantu, P. Brocca, Y. Gerelli, B. Demé, M. M. Koza, M. Johnson and J. Peters, *Eur. Phys. J. E: Soft Matter Biol. Phys.*, 2016, **39**, 1–10.
33 J. Teixeira, M. Bellissent-Funel, S. H. Chen and A. J. Dianoux, *Phys. Rev. A: At., Mol., Opt. Phys.*, 1985, **31**, 1913–1917.
34 T. Matsuo, A. Cisse, M. Plazanet, F. Natali, M. M. Koza, J. Ollivier, D. J. Bicout and J. Peters, *Biochim. Biophys. Acta, Biomembr.*, 2022, **1864**, 183949.
35 A. Cisse, T. Matsuo, M. Plazanet, F. Natali, M. M. Koza, J. Ollivier, D. J. Bicout and J. Peters, *Biochim. Biophys. Acta, Biomembr.*, 2022, **1864**, 183950.
36 J. P. Douliez, B. H. Houssou, A. L. Fameau, L. Navailles, F. Nallet, A. Grelard, E. J. Dufourc and C. Gaillard, *Langmuir*, 2016, **32**, 401–410.

